J|A|C|S
ARTICLES
Published on Web 03/12/2003

Discovery of a Potent, Selective Protein Tyrosine Phosphatase 1B Inhibitor Using a Linked-Fragment Strategy

Bruce G. Szczepankiewicz,* Gang Liu,[†] Philip J. Hajduk,[‡] Cele Abad-Zapatero,[‡] Zhonghua Pei,[†] Zhili Xin,[†] Thomas H. Lubben,[§] James M. Trevillyan,[§] Michael A. Stashko,[§] Stephen J. Ballaron,[§] Heng Liang,[‡] Flora Huang,[‡] Charles W. Hutchins,[‡] Stephen W. Fesik,[||] and Michael R. Jirousek[⊥]

Contribution from the Global Pharmaceutical Research and Development Organization, Abbott Laboratories, 100 Abbott Park Road, Abbott Park, Illinois 60064

Received December 10, 2002; E-mail: bruce.szczepankiewicz@abbott.com

Abstract: Protein tyrosine phosphatase 1B (PTP1B) is an enzyme that downregulates the insulin receptor. Inhibition of PTP1B is expected to improve insulin action, and the design of small molecule PTP1B inhibitors to treat type II diabetes has received considerable attention. In this work, NMR-based screening identified a nonselective competitive inhibitor of PTP1B. A second site ligand was also identified by NMR-based screening and then linked to the catalytic site ligand by rational design. X-ray data confirmed that the inhibitor bound with the catalytic site in the native, "open" conformation. The final compound displayed excellent potency and good selectivity over many other phosphatases. The modular approach to drug design described in this work should be applicable for the design of potent and selective inhibitors of other therapeutically relevant protein tyrosine phosphatases.

Introduction

Reversible protein phosphorylation is the predominant strategy used to control the activity of proteins in eucaryotic cells. Approximately 30% of the 10 000 proteins in a typical mammalian cell are thought to be phosphorylated.[1,2] Many cellular functions could be artificially manipulated if one could exogenously control the activity of protein kinases and phosphatases.[3] This has led to intense interest in identifying small molecules capable of inhibiting the action of specific kinases[4,5] or phosphatases.[6,7] Such agents offer a great deal of promise as new therapies for a wide variety of human diseases including cancer, inflammation, and diabetes.

Type II diabetes afflicts over 130 million people worldwide, and the incidence is expected to grow steadily over the next several years.[8] Current treatments include injectable insulin and oral hypoglycemic agents such as metformin, sulfonlyureas, the thiazolidinediones, and α-glucosidase inhibitors.[9] However, no combination of these therapies is completely successful in ameliorating type II diabetes for many patients, and more efficacious agents are needed. A major goal of new therapies for type II diabetes is to potentiate the action of insulin. One of the key proteins involved in insulin signaling is the insulin receptor. When insulin binds to its receptor, changes in the intracellular conformation of the receptor result in the *O*-phosphorylation of three specific tyrosine residues.[10] This serves as the first step in insulin signaling, and it is followed by a cascade of intracellular events that mediate the physiological effects of insulin.[11] There is compelling evidence that protein tyrosine phosphatase 1B, or PTP1B, is primarily responsible for the dephosphorylation of the insulin receptor and, therefore, acts to downregulate insulin signaling.[12−16] A PTP1B inhibitor would be expected to increase the half-life of the phosphorylated insulin receptor and enhance the effects of insulin. The most intriguing data to support this hypothesis come from the knockout mouse studies reported by two different laborato-

* Address correspondence to this author at R4MC AP10/LL12, Metabolic Disease Research, Abbott Laboratories, 100 Abbott Park Road, Abbott Park, IL 60064-6098. Phone: (847) 935-1559. Fax: (847) 938-1674.
[†] R4MC Metabolic Disease Research.
[‡] R46Y Advanced Technologies.
[§] R47R Metabolic Disease Research.
[||] R460 Cancer Research.
[⊥] Current address: Pfizer Global Research and Development, La Jolla Laboratories, 10770 Science Center Drive, San Diego, CA 92121.

(1) Alberts, B.; Bray, D.; Lewis, J.; Raff, M.; Roberts, K.; Watson, J. *Molecular Biology of the Cell*, 3rd ed.; Garland: New York, 1994; p 202.
(2) Cohen, P. *Trends Biochem. Sci*. **2000**, *25*, 596.
(3) Ahn, N. *Chem. Rev.* **2001**, *101*, 2207.
(4) Toledo, L. M.; Lydon, N. B.; Elbaum, D. *Curr. Med. Chem*. **1999**, *6*, 775.
(5) Rewcastle, G. W.; Denny, W. A.; Showalter, H. D. H. *Curr. Org. Chem*. **2000**, *4*, 679.
(6) Serine threonine phosphatase inhibitors: McCluskey, A.; Sim, A. T. R.; Sakoff, J. A. *J. Med. Chem.* **2002**, *45*, 1151.
(7) Protein tyrosine phosphatases: Zhang, Z.-Y. *Annu. Rev. Pharmacol. Toxicol.* **2002**, *42*, 209.
(8) Zimmet, P., Alberti, K. G. M. N.; Shaw, J. *Nature* **2001**, *414*, 782.
(9) Nuss, J. M.; Wagman, A. S. In *Annual Reports in Medicinal Chemistry*; Doherty, A. M., Ed.; Academic Press: San Diego, CA, 2000; Vol. 35, pp 211−220.
(10) Kahn, C. R. *Diabetes* **1994**, *43*, 1066.
(11) Czech, M. P.; Corvera, S. *J. Biol. Chem.* **1999**, *274*, 1865.
(12) Kenner, K. A.; Anyanwu, E.; Olefsky, J. M.; Kusari, J. *J. Biol. Chem.* **1996**, *271*, 19810.
(13) Chen, H.; Wertheimer, S. J.; Lin, C. H.; Katz, S. L.; Amrein, K. E.; Burn, P.; Quon, M. J *J. Biol. Chem.* **1997**, *272*, 8026.
(14) Ahmad, F.; Li, P. M.; Meyerovitch, J.; Goldstein, B. J. *J. Biol. Chem.* **1995**, *270*, 20503.
(15) Chen, H.; Cong, L. N.; Li, Y.; Yao, Z. J.; Wu, L.; Zhang, Z. Y.; Burke, T. R., Jr.; Quon, M. J. *Biochemistry* **1999**, *38*, 384.
(16) Walchli, S.; Curchod, M. L.; Gobert, R. P.; Arkinstall, S.; Hooft van Huijsduijnen, R. *J. Biol. Chem.* **2000**, *275*, 9792.

10.1021/ja0296733 CCC: $25.00 © 2003 American Chemical Society

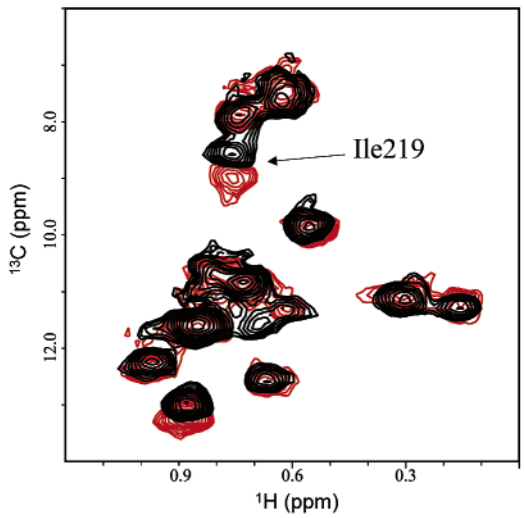

Figure 1. ^{13}C/^{1}H HSQC NMR spectra of δ-$^{13}CH_3$ Ile-labeled PTP1B in the absence (black) and presence (red) of 0.1 mM diaryloxamic acid **1**. Significant chemical shift perturbations in the δ-methyl resonance of Ile219 were observed upon addition of ligand.

ries.[17,18] PTP1B deficient mice were viable, healthy, and lean. They displayed enhanced insulin sensitivity and resistance to diet-induced obesity. This provides important evidence that PTP1B inhibition would be an effective diabetes therapy. The development of PTP1B inhibitors began in the early 1990s and continues today.[19−22]

In an effort to develop a small, potent, and selective PTP1B inhibitor, we used a combination of NMR-based screening and iterative structure-based drug design to identify and optimize a lead compound. This compound is a potent, competitive inhibitor of PTP1B with a novel binding mode that selectively inhibits PTP1B versus many other phosphatases.

Results and Discussion

Discovery of a Catalytic Site Ligand. To identify novel scaffolds that could be used in the design of potent PTP1B inhibitors, NMR-based screening of a 10,000 compound library was employed. Screening was accomplished using a truncated, 292 amino acid version of PTP1B either uniformly labeled with ^{15}N or selectively labeled with δ-$^{13}CH_3$ Ile. Ligand binding was monitored by observing chemical shift changes in ^{1}H/^{15}N or ^{1}H/^{13}C-HSQC in the presence of test compounds. [23,24] As shown in Figure 1, high-resolution HSQC spectra could be obtained on the protein, and ligand binding could be detected readily. The NMR screen identified diaryloxamic acid **1** as a ligand for

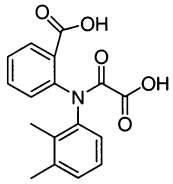

1

Figure 2. Structure of diaryloxamic acid **1**.

Scheme 1 [a]

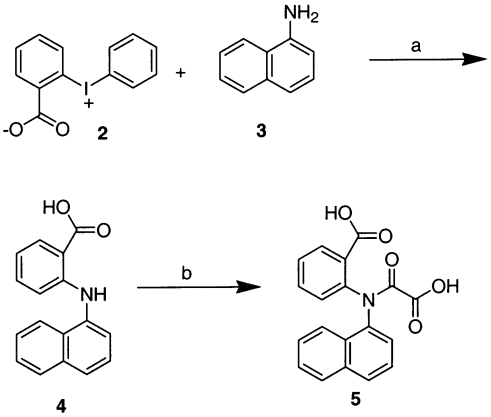

[a] Reagents and conditions: (a) $Cu(OAc)_2$, *i*-PrOH, reflux (43%); (b) (i) EtOCOCOCl, Et_3N, DMF, (ii) aqueous NaOH (16%).

PTP1B (Figure 2). This compound caused chemical shift changes similar to those for phosphotyrosine (pTyr). Significant perturbations in the ^{15}N amide resonances were observed for Val49, Gly220, and Gly 218 and also for the δ-$^{13}CH_3$ resonance of Ile219. In addition, the K_d value of compound **1** as measured by NMR ($K_d = 100\ \mu$M) compared favorably with the activity of this compound in a PTP1B-mediated *para*-nitrophenyl phosphate (*p*NPP) hydrolysis assay ($K_i = 293 \pm 174\ \mu$M). These data suggested that diaryloxamic acid **1** was binding to the active site of PTP1B and could serve as a pTyr mimetic for lead development. Two other groups have reported monoaryloxamates as phosphotyrosine surrogates.[25,26]

Improving the Catalytic Site Ligand. Reasoning that occupation of more space within the active site would lead to a more potent inhibitor, we prepared naphthyloxamic acid **5** via a three-step sequence (Scheme 1). NMR titration data yielded a K_d of 26 μM for naphthyloxamic acid **5**, which correlated well with the K_i value of $39 \pm 14\ \mu$M ($n = 3$) observed in the *p*NPP hydrolysis assay. The inhibition kinetics were consistent with competitive and reversible inhibition,[27] indicating that naphthyloxamic acid **5** did not form any covalent bonds to PTP1B and that it did not permanently alter PTP1B in any other way.

An X-ray structure of compound **5** bound to PTP1B was obtained which clearly showed how the inhibitor binds to the

(17) Elchebly, M.; Payette, P.; Michaliszyn, E.; Cromlish, W.; Collins, S.; Loy, A. L.; Normandin, D.; Cheng, A.; Himms-Hagen, J.; Chan, C. C.; Ramachandran, C.; Gresser, M. J.; Tremblay, M. L.; Kennedy, B. P. *Science* **1999**, *283*, 1544.
(18) Klaman, L. D.; Boss, O.; Peroni, O. D.; Kim, J. K.; Martino, J. L.; Zabotny, J. M.; Moghal, N.; Lubkin, M.; Kim, Y.-B.; Sharpe, A. H.; Stricker-Krongrad, A.; Shulman, G. I.; Neel, B. G.; Kahn, B. B. *Mol. Cell. Biol.* **2000**, *20*, 5479.
(19) Ripka, W. C. In *Annual Reports in Medicinal Chemistry*; Doherty, A. M., Ed.; Academic Press: San Diego, CA, 2000; Vol. 35, pp 231−250.
(20) Johnson, T. O.; Ermolieff, J.; Jirousek, M. *Nat. Rev. Drug Discovery* **2002**, *1*, 696.
(21) Blaskovich, M. A.; Kim, H.-O. *Expert Opin. Ther. Pat.* **2002**, *12*, 871.
(22) Shen, K.; Keng, Y.-F.; Wu, L.; Guo, X.-L.; Lawrence, D. S.; Zhang, Z.-Y. *J. Biol. Chem.* **2001**, *276*, 47311. Compound **40** in this work gave a K_i of 2.4 ± 0.2 nM for PTP1B.
(23) Shuker, S. B.; Hajduk, P. J.; Meadows, R. P.; Fesik, S. W. *Science* **1996**, *274*, 1531.
(24) Hajduk, P. J.; Augeri, D. J.; Mack, J.; Mendoza, R.; Yang, J.; Betz, S. F.; Fesik, S. W. *J. Am. Chem. Soc.* **2000**, *122*, 7898.
(25) (a) Iversen, L. F.; Andersen, H. S.; Møller, K. B.; Olsen, O. H.; Peters, G. H.; Branner, S.; Mortensen, S. B.; Hansen, T. K.; Lau, J.; Ge, Y.; Holsworth, D. D.; Newman, M. J.; Møller, N. P. H. *Biochemistry* **2001**, *40*, 14812. (b) Peters, G. H.; Iversen, L. F.; Branner, S.; Andersen, H. S.; Mortensen, S. B.; Olsen, O. H.; Møller, K. B.; Møller, N. P. H. *J. Biol. Chem.* **2000**, *275*, 18201. (c) Andersen, H. S.; Iversen, L. F.; Jeppesen, C. B.; Branner, S.; Norris, K.; Rasmussen, H. B.; Møller, K. B.; Møller, N. P. H. *J. Biol. Chem.* **2000**, *275*, 7101.
(26) Beaulieu, P. L.; Cameron, D. R.; Ferland, J.-M.; Gauthier, J.; Ghiro, E.; Gillard, J.; Gorys, V.; Poirier, M.; Rancourt, J.; Wernic, D.; Llinas-Brunet, M. *J. Med. Chem.* **1999**, *42*, 1757.
(27) Cornish-Bowden, A. *Fundamentals of Enzyme Kinetics*, revised ed.; Portland Press, Ltd.: London, 1995; Chapter 5.

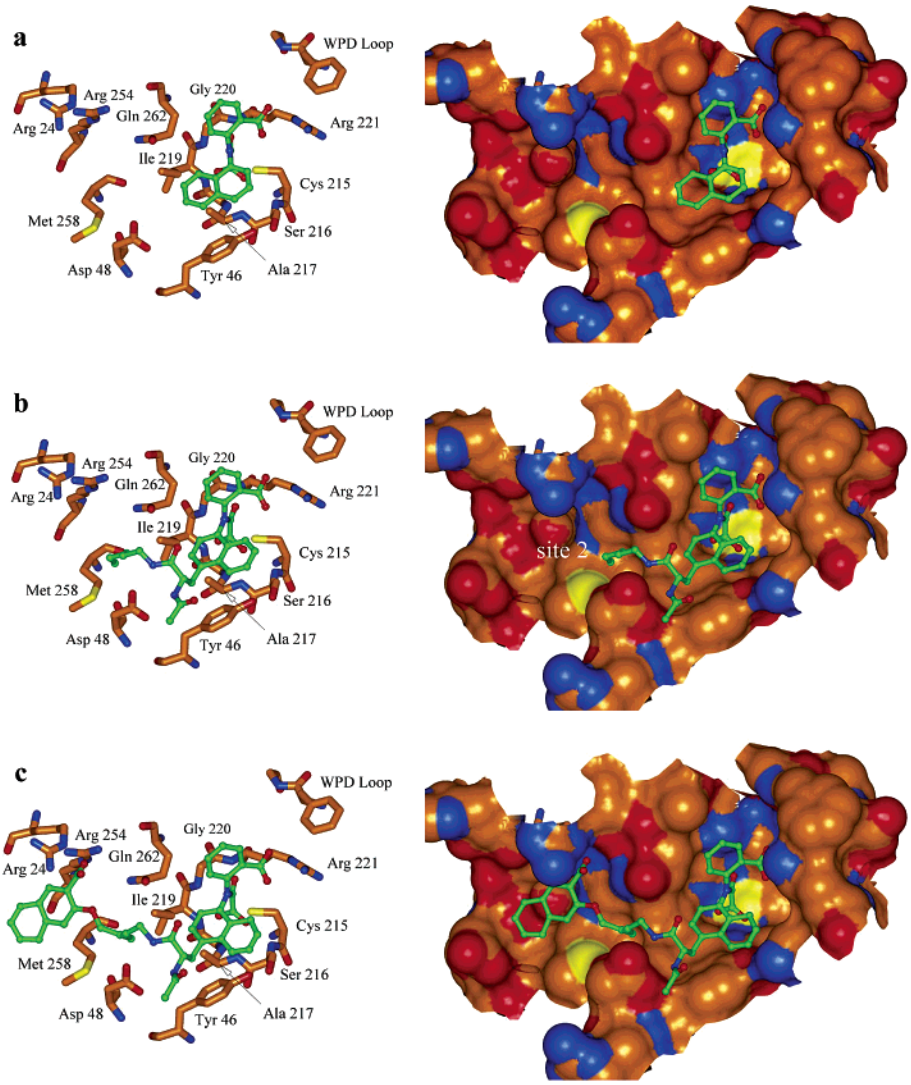

Figure 3. X-ray structures of PTP1B complexed with inhibitor **5** (a), inhibitor **12** (b), and inhibitor **23** (c). Protein color scheme: orange = carbon; red = oxygen; blue = nitrogen; yellow = sulfur. Inhibitor carbon atoms are shown in green.

active site of PTP1B (Figure 3a). Naphthyloxamic acid **5** binds to the "open" form of the enzyme, where the WPD loop (Trp179−Ser187) retains a conformation similar to the unoccupied enzyme.[28] This is different from that observed for most other inhibitors, where the WPD loop closes down toward the active site cysteine (Cys215).[29] As a result of binding to the open conformation, the naphthyloxamates have access to a much larger active site. The benzoic acid carboxylate group interacts with Arg221, and the benzene ring makes hydrophobic contacts with the side chain of Gln262. These critical interactions stabilize the open form of the enzyme and preclude the WPD loop from closing. The amide carbonyl oxygen and the oxanilic acid anion are positioned to form hydrogen bonds to a ring of backbone amides defined by the residues Ser216−Gly220. Another hydrophobic interaction between the naphthalene portion and Tyr46 also contributes to binding.

Installation of a Catalytic Site−Site 2 Linker. Despite its unusual binding mode, naphthyloxamic acid **5** showed some similarities to phosphotyrosine when bound to PTP1B. In particular, the phosphate and oxamate groups of the two compounds are similarly positioned, and the naphthalene system occupies the same region of the binding site as the benzene ring of phosphotyrosine[30] (Figure 4). The overlaid X-ray structures indicated that a diamide bearing chain might extend out of the active site from the 5-naphthyl position. Initial attempts to substitute the 5- or 6-naphthyl position resulted in the loss of inhibitory activity (data not shown). However, incorporation of a diamido chain at the 4-position gave compound **12** (Scheme 2) and resulted in nearly a 40-fold boost in potency, with a K_i value of 1.1 ± 0.5 μM. The active site contacts observed with compound **5** were preserved with inhibitor **12**, but the X-ray structure showed that the naphthyl ring system had flipped 180°. This ring flip occurs to accommodate two interactions between inhibitor **12** and PTP1B that are not possible with compound **5** (Figure 3b). The diamide chain extends out of the active site and reaches Asp48, where it forms two hydrogen bonds to the side chain carboxylate. The pentyl chain continues past Asp48 and is pointed directly toward

(28) Barford, D.; Flint, A. J.; Tonks, N. K. *Science* **1994**, *263*, 1397.
(29) Groves, M. R.; Yao, Z.-J.; Roller, P. P.; Burke, T. R., Jr.; Barford, D. *Biochemistry* **1998**, *37*, 17773.
(30) Salmeen, A.; Andersen, J. N.; Myers, M. P.; Tonks, N. K.; Barford, D. *Mol. Cell* **2000** *6*, 1401.

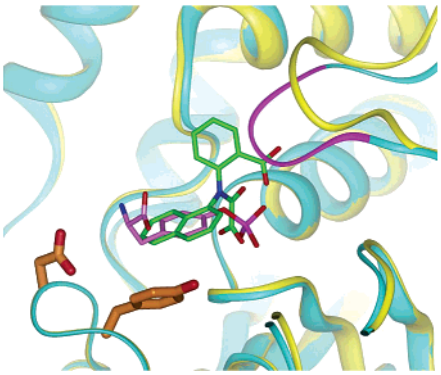

Figure 4. Overlay of the PTP1B (yellow ribbon)−naphthyloxamic acid **5** (green) complex with catalytically inactive PTP1B (Cys215Ser, cyan ribbon) bound to a phosphotyrosine residue (magenta). The WPD loop in the catalytically inactive protein ("closed" position) is shown in magenta. Asp48 and Tyr46 are highlighted in orange.

Scheme 2 [a]

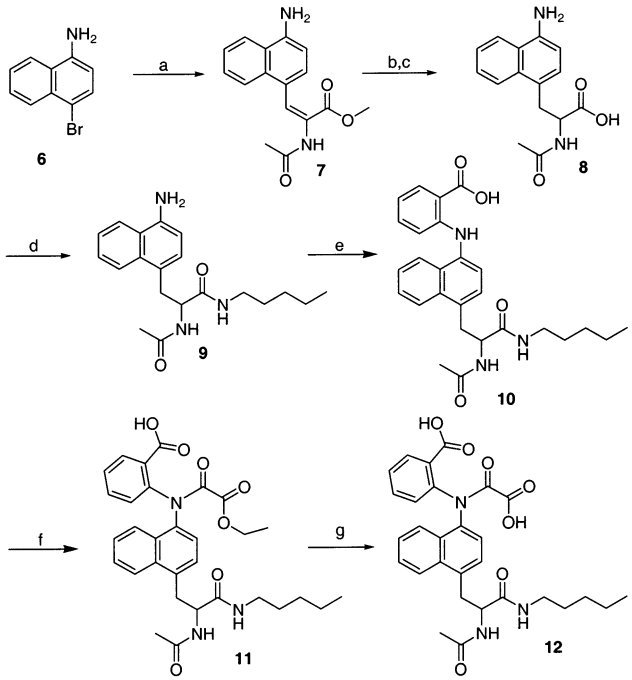

[a] Reagents and conditions: (a) methyl 2-acetamidoacrylate, $Pd(OAc)_2$, $P(o\text{-tolyl})_3$, Et_3N, DMF, 110 °C (76%); (b) 10% Pd/C, *i*-PrOH, 4 atm of H_2 (100%); (c) 3 N aqueous NaOH, MeOH, 25 °C (74%); (d) TBTU, HOBT, amylamine, Et_3N, DMF, (88%); (e) **2** (see Scheme 1), $Cu(OAc)_2$, *i*-PrOH, 80 °C (83%), (f) $ClCOCO_2Et$, *i*-Pr_2NEt, CH_2Cl_2, 0 °C → 25 °C; (g) NaOH, EtOH, 25 °C (29%).

a second, noncatalytic phosphotyrosine binding site (site 2).[31] Thus, the diamide linkage not only imparted additional binding energy but also served as a bridge between the catalytic and noncatalytic binding sites.

Discovery and Incorporation of a Site 2 Ligand. Accessing the noncatalytic phosphotyrosine binding region was an important goal. The catalytic domain is generally conserved among many tyrosine phosphatases, so achieving selectivity for PTP1B over other phosphatases was likely to be difficult without also accessing a region outside the active site. As first reported by Zhang and Lawrence, the second, noncatalytic site is much less homologous among different tyrosine phosphatases and so

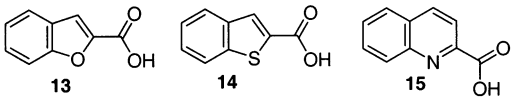

Figure 5. Selected PTP1B site 2 ligands identified using NMR screening.

represents a region that could impart enzyme selectivity.[31] Thus, the next stage in the design strategy was to utilize the diamide bridge to position groups in the noncatalytic site that would not only improve the potency but also impart greater PTP1B specificity to the series.

NMR screening was again utilized to identify a ligand for site 2. Binding to the noncatalytic site was specifically monitored by labeling the protein with ^{13}C-methionine and following the resonance of Met258, an amino acid present in site 2 (see Figure 3b).[24] Screening 10,000 compounds identified several capable of binding weakly (K_d > 1 mM) to this site. Many of these ligands were small fused-ring aromatic acids, such as 2-benzofurancarboxylic acid (**13**), 2-benzothiophenecarboxylic acid (**14**), or 2-quinolinecarboxylic acid (**15**) (Figure 5). Having two ligands that bound to proximal sites on the protein along with a suitable linker provided a straightforward application of the linked-fragment SAR-by-NMR approach.[23] The nature of the site 2 ligands identified by screening implied that a naphthoic acid might also be a suitable site 2 ligand. Since 3-hydroxy-2-naphthoic acid methyl ester (**18**) could easily be linked to compound **12**, inhibitor **23** was prepared according to the route depicted in Scheme 3. Whereas compound **12** was racemic, inhibitor **23** was prepared with complete stereocontrol starting from *N*-Boc-(*S*)-3-iodoalanine methyl ester.

The K_i for inhibitor **23** was 22 ± 6 nM (n = 3). The second site ligand therefore gave a 25-fold improvement in inhibitory activity, with a concurrent 2-fold improvement from the asymmetric catalytic site ligand. The conformations of the naphthyloxamate and diamide linker regions of inhibitor **23** were essentially identical to those of compound **12**, and the naphthoic acid was positioned in site 2 (Figure 3c). The naphthoic acid carboxylate group was positioned 2.6 Å from Arg254 and 2.8 Å from Arg24. Either or perhaps both Arg residues could therefore be participating in a salt bridge or H-bonding interaction with the naphthoic acid. The naphthalene system forms a weak (4.1 Å) hydrophobic interaction with Met258.

Selectivity Against Other Phosphatases. To determine the selectivity of the new compounds, we measured their inhibitory activity against a panel of several phosphatases including CD45,[32] LAR,[33] SHP-2,[34] calcineurin,[35] and TCPTP.[36] On the basis of amino acid sequence homology, TCPTP is the phosphatase most closely related to PTP1B. Selectivity for PTP1B over TCPTP inhibition would therefore represent the highest level of specificity for the desired phosphatase over another.

The K_i values of inhibitors **1**, **5**, **12**, and **23** against the phosphatases tested are shown in Table 1, and selectivity ratios are given in Table 2. Inhibitor **5** showed similar activity against PTP1B (K_i = 39 ± 14 μM), TCPTP (K_i = 44 ± 8 μM), and LAR (K_i = 34.8 ± 1.6 μM). This compound showed little or

(31) Puius, Y. A.; Zhao, Y.; Sullivan, M.; Lawrence, D. S.; Almo, S. C.; Zhang, Z.-Y. *Proc. Natl. Acad. Sci. U.S.A.* **1997**, *94*, 13420.
(32) Penninger, J. M.; Irie-Sasaki, J.; Sasaki, T.; Oliveira-dos-Santos, A. J. *Nat. Immunol.* **2001**, *2*, 389.
(33) Cheng, A.; Dube, N.; Gu, F.; Trembley, M. L. *Eur. J. Biochem.* **2002**, *269*, 1050.
(34) Qu, C.-K. *Biochim. Biophys. Acta* **2002**, *1592*, 297.
(35) Rusnak, F.; Mertz, P. *Physiol. Rev.* **2000**, *80*, 1483.
(36) Ibarra-Sanchez, M.d. J.; Simoncic, P. D.; Nestel, F. R.; Duplay, P.; Lapp, W. S.; Trembley, M. L. *Semin. Immunol.* **2000**, *12*, 379.

Scheme 3 [a]

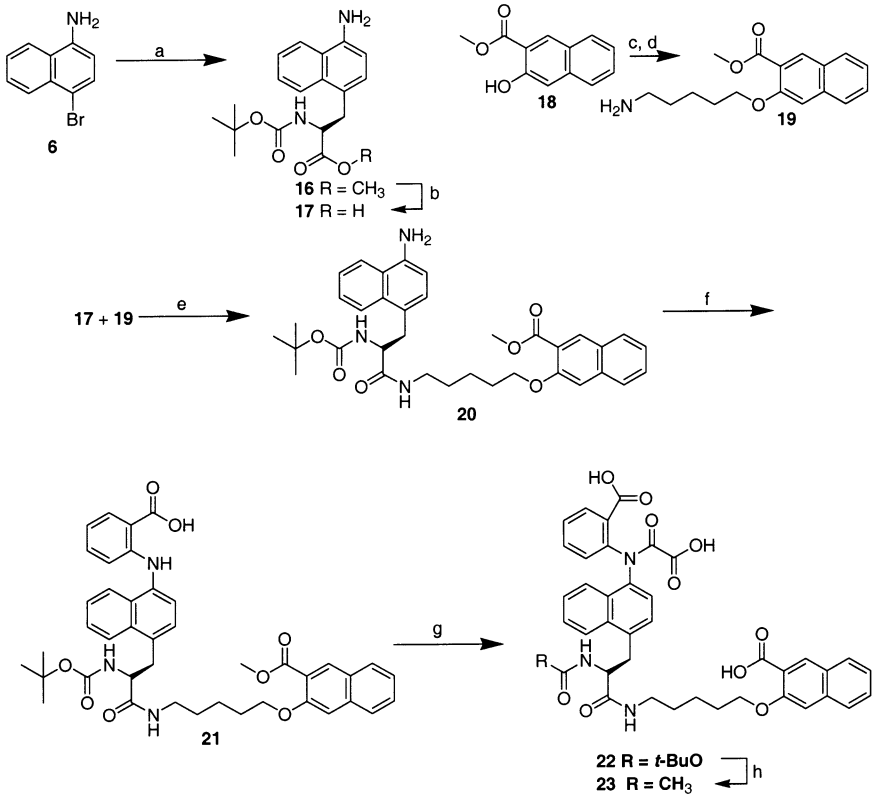

[a] Reagents and conditions: (a) (i) *N*-Boc-(*S*)-3-iodoalanine, Zn, DMF, (ii) $Pd(OAc)_2$, *o*-tol_3P, **6** (55%); (b) NaOH, aqueous CH_3OH (83%); (c) *N*-Boc-5-amino-1-pentanol, PPh_3, DEAD, THF (56%); (d) 4 M HCl, dioxane (95%); (e) EDCI, HOBT, NMM, CH_2Cl_2 (90%); (f) DPIC (**2**), $Cu(OAc)_2$, *i*-PrOH (100%); (g) (i) EtOCOCOCl, Et_3N, DMF, (ii) aqueous NaOH; (h) (i) CF_3COOH, (ii) aqueous NaOH, (iii) Ac_2O (28%).

Table 1. K_i of Inhibitors **1**, **5**, **12**, and **23** against Various Phosphatases[a]

	compd			
phosphatase	**1**	**5**	**12**	**23**
PTP1B	293 ± 175 (3)	39 ± 14 (3)	1.1 ± 0.5 (6)	0.022 ± 0.006 (3)
TCPTP	164 ± 36 (2)	44 ± 8 (2)	1.1 ± 0.9 (3)	0.049 ± 0.006 (3)
LAR	>900 (2)	34.8 ± 1.6 (2)	6.7 ± 4.7 (4)	1.3 ± 0.5 (2)
SHP-2	>900 (2)	>300 (2)	29.6 ± 3.6 (2)	2.49 ± 0.19 (2)
CD45	>360 (2)	176 (1)	417 ± 271 (7)	53.6 ± 5.7 (2)
calcineurin		>300 (2)	>300 (2)	>300 (2)

[a] K_i values are in units of μM ± standard deviation, with the number of determinations in parentheses.

Table 2. Selectivity Ratios for Inhibitors **1**, **5**, **12**, and **23** over Various Phosphatases

	compd			
phosphatase	**1**	**5**	**12**	**23**
PTP1B	1	1	1	1
TCPTP	1	1	1	2
LAR	>3	1	6	36
SHP-2	>3	>7	27	104
CD45	>1	>4	380	2700
calcineurin		>7	>270	>13000

no activity against SHP-2 (K_i > 300 μM), CD45 (K_i > 176 μM), and calcineurin (K_i > 300 μM). Inhibitor **12** showed similar activity against PTP1B ($K_i = 1.1 \pm 0.5\ \mu$M) and TCPTP ($K_i = 1.1 \pm 0.9\ \mu$M) but modest selectivity over LAR ($K_i = 6.7 \pm 4.7\ \mu$M). Selectivity for inhibitor **12** was good over SHP-2 ($K_i = 29.6 \pm 3.6\ \mu$M), CD45 ($K_i = 417 \pm 271\ \mu$M), and calcineurin (K_i > 300 μM). As we had hoped, inhibitor **23** proved to be the most PTP1B selective inhibitor. This compound showed modest but significant selectivity for PTP1B ($K_i = 22 \pm 6$ nM) over TCPTP ($K_i = 49 \pm 6$ nM). Inhibitory activity against LAR ($K_i = 1.3 \pm 0.5\ \mu$M), SHP-2 ($K_i = 2.49 \pm 0.19\ \mu$M), CD45 ($K_i = 53.6 \pm 5.7\ \mu$M), and calcineurin (K_i > 300 μM) demonstrated excellent selectivity for PTP1B.

The inhibitory data for compound **23** vindicated the hypothesis that PTP1B selectivity against closely related phosphatases was possible by taking advantage of the site 2 interactions. We did not have access to the crystal structure of TCPTP,[37] but a homology model indicated that TCPTP also bore a second phosphotyrosine binding site similar to the PTP1B second site. In particular, Arg254 and Arg24 are conserved between PTP1B and TCPTP (see Figure 3c). However, the exact shape of the second site is expected to vary because of two point mutations, Cys32 in PTP1B to His32 in TCPTP and Phe52 in PTP1B to Tyr52 in TCPTP. We believe that the differences in the second site alter the interaction of the naphthoic acid with the two arginine residues, affording some selectivity for PTP1B over

(37) Iversen, L. F.; Møller, K. B.; Pedersen, A. K.; Peters, G. H.; Petersen, A. S.; Andersen, H. S.; Branner, S.; Mortensen, S. B.; Møller, N. P. H. *J. Biol. Chem.* **2002**, *277*, 19982.

TCPTP. We also observed a modest improvement in inhibition of LAR and CD45 upon installation of the site 2 ligand on an asymmetric core, while we saw a more substantial improvement in activity against SHP-2. These data indicate that the naphthoic acid may make some binding contacts with each of these phosphatases, albeit to widely varying degrees. Modification of the second site ligand, or alternate second site ligands, could result in still better selectivity for PTP1B.

Conclusion

Starting with low affinity leads from NMR-based screening, the inhibitor series was incrementally constructed by fully utilizing the structural and NMR screening data to rationally improve both potency and selectivity. Compound **23** is among the most potent nonpeptidic PTP1B inhibitors reported to date, and it displays excellent selectivity against LAR, SHP-2, CD-45, and calcineurin. The modest selectivity against TCPTP is noteworthy given the extremely high sequence identity between these two phosphatases. It is also interesting that while the site 2 ligand endowed compound **23** with improved selectivity for PTP1B, it also improved inhibitory activity to a lesser extent against TCPTP and SHP-2. Since these phosphatases appear to accommodate a second site ligand, it is possible that selectivity for these and other tyrosine phosphatases can be achieved by choosing an appropriate second site ligand for each. The NMR screening method we employed to discover a PTP1B selective site 2 ligand could serve to find selective, noncatalytic site ligands for other tyrosine phosphatases as well. Such a strategy could greatly reduce the discovery time for identifying specific tyrosine phosphatase inhibitors. These inhibitors would be useful tools to probe the role of phosphatases in different cellular processes and may ultimately lead to new therapeutic agents for many human diseases.

Experimental Section

Chemistry. General Methods. Reactions were dried over $MgSO_4$ or Na_2SO_4, filtered through a fritted glass funnel or a plug of cotton, and concentrated with a rotary evaporator at ca. 15 mmHg, warming when necessary. Thin-layer chromatography systems were the same as those used for column chromatography, with R_f approximately 0.3. Thin-layer chromatography was performed using Merck F-254 silica gel plates. Column chromatography was performed under 5 psi N_2 using 230−400 mesh silica gel. Analytical HPLC traces and compounds purified by HPLC were obtained by elution through a C_{18} reverse-phase column with a gradient of 5 mM aqueous ammonium acetate/acetonitrile or 0.1% aqueous TFA/acetonitrile as eluants. Concentration gradients started at 0% acetonitrile and 100% aqueous medium. Starting materials were obtained from commercial suppliers and used without further purification. ^{1}H NMR data are tabulated in the following order: multiplicity (s, singlet; d, doublet, t, triplet; m, multiplet, b, broad), number of protons, coupling constants in hertz. Where mixtures of stereoisomers or rotamers were obtained, the ^{1}H NMR resonances of the major species are reported, unless otherwise indicated.

2-[(2,3-Dimethylphenyl)oxalylamino]benzoic acid (1). (An alternate route to oxamic acid **2** has been described previously.[38]) To 1.21 g (10.0 mmol) of 2,3-dimethylaniline, 3.42 g (10.0 mmol) of diphenyliodonium-2-carboxylate monohydrate (**2**), and 73 mg (0.40 mmol) of copper(II) acetate was added 40 mL of 2-propanol. The mixture was stirred at reflux under N_2 for 23 h and then concentrated in vacuo. The solid residue was taken up in 100 mL of ethyl acetate, with gentle heating to aid dissolution. The solution was extracted with water (2 × 25 mL) and brine (1 × 25 mL), dried over $MgSO_4$, filtered, and concentrated to a solid. This was recrystallized from 40 mL of ethyl acetate to give 1.3 g (54%) of 2-((2,3-dimethylphenyl)amino)benzoic acid[39] as colorless crystals: ^{1}H NMR (400 MHz, DMSO-d_6) δ 12.95 (bs, 1H), 9.44 (bs, 1H), 7.89 (d, 1H, J = 7.1 Hz), 7.30 (t, 1H, J = 7.2 Hz), 7.11 (m, 2H), 7.03 (t, 1H, J = 4.5 Hz), 6.69 (m, 2H), 2.29 (s, 3H), 2.10 (s, 3H); ^{13}C NMR (100 MHz, DMSO-d_6) δ 170.1 (C), 148.7 (C), 138.3 (C), 137.8 (C), 134.1 (CH), 131.7 (CH), 131.2 (C), 126.3 (CH), 125.9 (CH), 122.1 (CH), 116.2 (CH), 113.0 (CH), 111.2 (C), 20.1 (CH_3), 13.6 (CH_3); MS (ESI) m/z 242 ($[M + H]^+$).

To an ice cooled solution of 2-((2,3-dimethylphenyl)amino)benzoic acid (343 mg, 1.55 mmol) and triethylamine (503 μL, 3.56 mmol) in dichloromethane (5 mL) was added ethyl oxalyl chloride (401 μL, 3.56 mmol) over 30 min. The reaction was warmed to ambient temperature and stirred for 16 h. The reaction mixture was then treated with 1 M HCl (10 mL) and extracted with dichloromethane (2 × 15 mL). The combined extracts were washed with brine, dried over Na_2SO_4, filtered, and concentrated in vacuo. The residue was dissolved in 5 mL of methanol, and 4.5 mL (4.5 mmol) of 1 M NaOH(aq) was added. After being stirred for 2 h at ambient temperature, the basic reaction mixture was diluted with 1 M HCl (10 mL). The product was isolated via reverse phase HPLC to provide 235 mg (48%) of 2-[(2,3-dimethylphenyl)-oxalylamino]benzoic acid (**1**) as a light brown solid: ^{1}H NMR (300 MHz, DMSO-d_6) mixture of rotamers δ 8.21 (dd, 1H [minor], J = 8.1, 1.0), 8.17 (d, 0.5H, J = 6.6 Hz), 8.05 (dd, 0.5, J = 7.7, 1.5 Hz), 7.94 (dd, 1H [minor], J = 7.7, 1.8 Hz), 7.81−7.22 (m, 5.5H), 7.07 (d, 0.5H, J = 7.3 Hz), 6.90 (d, 1H [minor], J = 8 Hz), 2.54 (s, 1.5H), 2.51 (s, 3H [minor]), 2.49 (s, 1.5H), 2.45 (s, 1.5H), 2.42 (s, 1.5H), 2.33 (s, 3H [minor]), 2.29 (s, 3H [minor]); ^{13}C NMR (100 MHz, DMSO-d_6) δ 167.1 (C), 166.5 (C), 163.3 (C), 162.0 (C), 140.5 (C), 140.2 (C), 139.2 (C), 138.6 (C), 138.4 (C), 137.7 (C), 135.2 (C), 134.0 (C), 133.2 (CH), 132.4 (C), 132.2 (CH), 131.3 (CH), 130.2 (CH), 130.1 (CH), 130.0 (CH), 129.1 (CH), 129.0 (C), 128.9 (CH), 128.1 (C), 127.7 (CH), 127.5 (CH), 126.5 (CH), 126.1 (CH), 125.5 (CH), 125.1 (CH), 20.1 (CH_3), 20.0 (CH_3), 14.5 (CH_3); MS (ESI) m/z 314 ($[M + H]^+$), 331 ($[M + NH_4]^+$), 336 ($[M + Na]^+$).

2-(Naphthalen-1-ylamino)benzoic Acid (4). To 3.42 g (10.0 mmol) of diphenyliodonium-2-carboxylate monohydrate (**2**), 1.43 g (10.0 mmol) of 1-aminonaphthalene (**3**), and 73 mg (0.40 mmol) copper(II) acetate was added 40 mL of 2-propanol. The mixture was stirred at reflux under N_2 for 2.5 h and then concentrated in vacuo. The solid residue was taken up in 100 mL of ethyl acetate and extracted with water (1 × 25 mL) and brine (1 × 25 mL), dried over $MgSO_4$, filtered, and concentrated to a solid. This was recrystallized from 20 mL of ethyl acetate to give 1.12 g (43%) of a gray solid: ^{1}H NMR (300 MHz, DMSO-d_6) δ 10.05 (bs, 1H), 7.98 (m, 3H), 7.78 (m, 1H), 7.55 (m, 4H), 7.33 (td, 1H, J = 7.3, 1.0 Hz), 6.92 (d, 1H, J = 8.5 Hz), 6.77 (t, 1H, J = 7.5 Hz); ^{13}C NMR (100 MHz, DMSO-d_6) δ 148.7 (C), 136.2 (C), 134.4 (C), 134.2 (CH), 131.9 (CH), 128.6 (C), 128.4 (CH), 126.3 (CH), 126.1 (CH), 124.5 (CH), 121.8 (CH), 119.7 (CH), 117.1 (CH), 113.8 (CH); MS (ESI) m/z 264 ($[M + H]^+$).

2-(Naphthalen-1-yloxalylamino)benzoic Acid (5). To an ice-cooled solution of 100 mg (0.380 mmol) of 2-(naphthalen-1-ylamino)benzoic acid (**4**) in 2 mL of DMF was added 400 μL (2.87 mmol) of triethylamine and then 200 μL (1.79 mmol) of ethyl chlorooxoacetate. The ice bath was removed, and the reaction was stirred at ambient temperature. After 2 h, 3 mL of 2 M NaOH(aq) was added, the solution was diluted with 10 mL water, and the mixture was allowed to stir for 2 h. Another 10 mL of water was added to clear the solution, and then the reaction was stirred for an additional 2 h. The mixture was treated with 3 mL of 6 M HCl and extracted with ethyl acetate (3 × 5 mL). The combined ethyl acetate layers were back-extracted with water (2 × 5 mL) and brine (1 × 5 mL), dried over $MgSO_4$, filtered, and

(38) Parke, Davis and Co. U.S. Patent No. 3238201, 1966.

(39) Scherrer, R. A.; Beatty, H. R. *J. Org. Chem.* **1980**, *45*, 2127.

concentrated to an oil. The product was purified via reverse phase HPLC, eluting with a gradient of 0−70% acetonitrile in 0.1% (v/v) aqueous trifluoroacetic acid. Product-containing fractions were concentrated in vacuo below 40 °C to give 54 mg (16%) of a white powder: ^{1}H NMR (3:2 mixture of rotamers) (500 MHz, DMSO-d_6) δ 8.37 (d, 1H, J = 8.7 Hz), 8.05−8.03 (m, 1H), 8.01−7.95 (m, 1H), 7.87 (dd, 1H, J = 1.8, 7.7 Hz), 7.68−7.73 (m, 1H), 7.63−7.59 (m, 1H), 7.57−7.49 (m, 2H), 7.45−7.38 (m, 1H), 7.34 (dt, 1H, J = 1.1, 7.5 Hz), 7.21 (d, 1H (rotamer), J = 7.7 Hz), 6.89 (d, 1H, J = 7.3 Hz); ^{13}C NMR (100 MHz, DMSO-d_6) δ 167.5 (C), 166.8 (C), 163.6 (C), 163.3 (C), 162.4 (C), 141.6 (C), 138.6 (C), 138.3 (C), 136.5 (C), 134.4 (C), 134.1 (C), 133.4 (CH), 132.3 (CH), 131.5 (CH), 130.3 (CH), 130.1 (C), 129.6 (CH), 129.5 (C), 129.0 (C), 128.7 (CH), 128.5 (CH), 128.4 (CH), 128.2 (CH), 128.2 (CH), 128.1 (CH), 127.3 (CH), 126.8 (CH), 126.8 (CH), 126.5 (CH), 126.0 (CH), 125.9 (CH), 125.6 (CH), 125.3 (CH), 123.9 (CH), 122.9 (CH); MS (ESI) m/z 336 ([M + H]$^+$), 353 ([M + NH$_4$]$^+$), 358 ([M + Na]$^+$).

2-(Acetylamino)-3-(4-aminonaphthalen-1-yl)acrylic Acid Methyl Ester (7). To a mixture of 4-bromo-1-naphthylamine (**6**) (2.5 g, 11.3 mmol), Pd(OAc)$_2$ (140 mg, 0.63 mmol), and P(*o*-tolyl)$_3$ (570 mg, 1.87 mmol) in anhydrous *N*,*N*-dimethylformamide (10 mL) in a pressure tube was added methyl 2-acetamidoacrylate (2.1 g, 14.7 mmol) and triethylamine (5.3 mL, 37.5 mmol).[40] The mixture was flushed with nitrogen for 3 min and then sealed and heated at 110 °C for 4 h. The reaction mixture was cooled to ambient temperature and then partitioned between ethyl acetate and water. The aqueous layer was extracted once with ethyl acetate, and the combined organic layers were washed with brine, dried (Na_2SO_4), filtered, and concentrated in vacuo. The crude residue was purified via silica gel chromatography, eluting with ethyl acetate to provide 2.5 g (76%) of compound **7** as a yellow solid: ^{1}H NMR (400 MHz, DMSO-d_6) δ 9.34 (s, 1H), 8.15 (d, 1H, J = 8.0 Hz), 7.90 (d, 1H, J = 8.0 Hz), 7.78 (s, 1H), 7.63 (d, 1H, J = 8.0 Hz), 7.51 (t, 1H, J = 7.6 Hz), 7.42 (t, 1H, J = 7.6 Hz), 6.72 (d, 1H, J = 8.0 Hz), 6.29 (s, 2H), 3.73 (s, 3H), 1.94 (s, 3H); ^{13}C NMR (100 MHz, DMSO-d_6) δ 169.4, 166.0, 147.1, 136.2, 129.4, 129.2, 126.7, 123.8, 123.4, 122.9, 122.1, 116.4, 106.9, 51.9, 22.4; MS (ESI) m/z 285 ([M + H]$^+$).

2-(Acetylamino)-3-(4-aminonaphthalen-1-yl)propionic Acid (8). To a solution of 2-acetylamino-3-(4-aminonaphthalen-1-yl)acrylic acid methyl ester (**7**) (2.5 g, 8.8 mmol) in 1:1 (v/v) ethyl acetate/methanol (50 mL) under N_2 was added Pd/C (10%, 250 mg). The reaction flask was capped with a hydrogen balloon and heated at 60 °C for 18 h. The mixture was filtered through diatomaceous earth, and the filter bed was washed with 1:1 (v/v) ethyl acetate/methanol (2 × 25 mL). The filtrate was concentrated in vacuo to provide the propoinate methyl ester (2.5 g, 100%). The methyl ester was dissolved in methanol (50 mL), and then 3 N NaOH (4.75 mL, 14.3 mmol) was added dropwise. After the reaction was stirred for 3 h at ambient temperature, the methanol was removed in vacuo, and then the remaining aqueous solution was acidified to pH ∼ 4.5 with 3 N HCl. The mixture was concentrated to dryness in vacuo, taken up in 10% (v/v) ethanol/dichloromethane (25 mL), and filtered through diatomaceous earth. The filter cake was washed with additional 10% (v/v) methanol/dichloromethane (10%, 25 mL). The filtrate was concentrated under reduced pressure to provide acid **8** as a brown solid (1.75 g, 74%): ^{1}H NMR (400 MHz, DMSO-d_6) δ 8.17 (d, 1H, J = 8.0 Hz), 8.08 (d, 1H, J = 8.0 Hz), 7.99 (d, 1H, J = 8.0 Hz), 7.48 (t, 1H, J = 7.8 Hz), 7.38 (t, 1H, J = 7.8 Hz), 7.12 (d, 1H, J = 7.8 Hz), 6.60 (d, 1H, J = 7.8 Hz), 1.77 (s, 3H), 4.45 (td, 1H, J = 4.8, 9.2 Hz), 3.43 (dd, 1H, J = 4.8, 14.0 Hz), 3.05 (dd, 1H, J = 9.2, 14.0 Hz); ^{13}C NMR (100 MHz, DMSO-d_6) δ 173.8, 169. 3, 143.8, 132.3, 128.3, 125.7, 123.4, 123.3, 123.0, 120.7, 107.1, 53.6, 34.3, 22.4; MS (ESI) m/z 273 ([M + H]$^+$).

2-(Acetylamino)-3-(4-aminonaphthalen-1-yl)-*N*-pentylpropionamide (9). A solution of 2-acetylamino-3-(4-aminonaphthalen-1-yl)-propionic acid (**8**) (500 mg, 1.84 mmol), 1-[3-(dimethylamino)propyl]-3-ethylcarbodiimide hydrochloride (EDCI) (493 mg, 2.57 mmol), 1-hydroxybenzotriazole hydrate (360 mg, 2.21 mmol), and *n*-pentylamine (320 μL, 2.75 mmol) in anhydrous *N*,*N*-dimethylformamide (10 mL) was adjusted to pH ∼6 by the addition of triethylamine, and then the reaction was stirred for 5 h at ambient temperature. The reaction was diluted with water and extracted with ethyl acetate (3 × 15 mL). The combined ethyl acetate layers were washed with water and then brine, dried over Na_2SO_4, filtered, and concentrated in vacuo. The product was purified via silica gel chromatography, eluting with 5% (v/v) MeOH/EtOAc to provide amide **9** as a yellow solid (552 mg, 1.62 mmol, 88%): ^{1}H NMR (400 MHz, DMSO-d_6) δ 8.15 (d, 1H, J = 8.0 Hz), 8.07 (s, 1H), 8.04 (s, 1H), 7.87 (t, 1H, J = 5.9 Hz), 7.45 (t, 1H, J = 8.0 Hz), 7.36 (t, 1H, J = 8.0 Hz), 7.08 (d, 1H, J = 8.0 Hz), 6.58 (d, 1H, J = 8.0 Hz), 5.52 (s, 2H), 4.27 (q, 1H, J = 5.9 Hz), 3.28 (dd, 1H, J = 5.9, 14.0 Hz), 2.94−3.06 (m, 3H), 1.77 (s, 3H), 1.18−1.39 (m, 4H), 1.14 (heptet, 2H, J = 7.8 Hz), 0.84 (t, 3H, J = 7.5 Hz); ^{13}C NMR (100 MHz, DMSO-d_6) δ 171.1, 169.0, 143.6, 132.4, 128.2, 125.4, 123.9, 123.1, 122.8, 120.7, 107.0, 54.0, 38.9, 38.4, 35.0, 28.5, 28.5, 22.5, 21.8, 13.9; MS (ESI) m/z 342 ([M + H]$^+$).

2-[(4-(2-(Acetylamino)-2-(pentylcarbamoyl)ethyl)naphthalen-1-yl)amino]benzoic Acid (10). To a stirred suspension of 2-(acetylamino)-3-(4-aminonaphthalen-1-yl)-*N*-pentylpropionamide (**9**) (552 mg, 1.62 mmol) and diphenyliodonium-2-carboxylate monohydrate (**2**) (580 mg, 1.78 mmol) in *N*,*N*-dimethylformamide (10 mL) was added anhydrous Cu(OAc)$_2$ (14.6 mg, 0.081 mmol). The mixture was heated at 95 °C for 1.5 h. The reaction mixture was then concentrated in vacuo, and the crude residue was purified by reverse phase preparative HPLC to give benzoic acid **10** as a light brown solid (619 mg, 83%): ^{1}H NMR (400 MHz, DMSO-d_6) δ 13.11 (s, 1H), 9.94 (s, 1H), 8.29 (d, 1H, J = 8.4 Hz), 8.18 (d, 1H, J = 8.4 Hz), 7.98 (d, 1H, J = 8.4 Hz), 7.94 (dd, 1H, J = 1.2, 7.6 Hz), 7.86 (t, 1H, J = 5.9 Hz), 7.61 (t, 1H, J = 7.6 Hz), 7.54 (t, 1H, J = 7.6 Hz), 7.41 (d, 1H, J = 7.6 Hz), 7.37 (d, 1H, J = 7.6 Hz), 7.26 (td, 1H, J = 1.2, 7.6 Hz), 6.78 (d, 1H, J = 8.4 Hz), 6.73 (t, 1H, J = 5.9 Hz), 4.59 (q, 1H, J = 7.6 Hz), 3.42 (dd, 2H, J = 7.2, 13.6 Hz), 3.23 (dd, 1H, J = 7.6, 14.0 Hz), 3.03 (qd, 1H, J = 7.6, 14.0 Hz), 2.91 (heptet, 1H, J = 6.4 Hz), 1.81 (s, 3H), 1.13−1.37 (m, 4H), 1.07 (heptet, 2H, J = 5.9 Hz), 0.79 (t, 3H, J = 5.9 Hz); ^{13}C NMR (100 MHz, DMSO-d_6) δ 170.5, 170.3, 169.1, 149.0, 135.0, 134.1, 132.9, 131.7, 130.9, 129.2, 127.5, 126.3, 125.9, 124.7, 122.5, 120.0, 116.7, 113.6, 111.7, 53.8, 38.5, 35.3, 28.5, 28.4, 22.5, 21.7, 13.8; MS (ESI) m/z 462 ([M + H]$^+$), 484 ([M + Na]$^+$).

***N*-Acetyl-4-[(carboxycarbonyl)(2-carboxyphenyl)amino]-*N*-pentyl-1-naphthylalaninamide (12).** To an ice-cooled, stirred solution of 2-[(4-(2-(acetylamino)-2-(pentylcarbamoyl)ethyl)naphthalen-1-yl)amino]benzoic acid (**10**) (619 mg, 1.34 mmol) and triethylamine (680 μL, 5.13 mmol) in dichloromethane (10 mL) was added ethyl oxalyl chloride (452 μL, 4.04 mmol) slowly, over 30 min. The reaction was warmed to ambient temperature and stirred for 16 h. After this time, 1 N HCl (10 mL) was added, and the mixture was extracted with dichloromethane (2 × 20 mL). The combined dichloromethane layers were washed with brine, dried over Na_2SO_4, filtered, and concentrated in vacuo. Crude ester **11** was hydrolyzed without any further purification.

To a solution of crude 2-{[4-(2-(acetylamino)-2-(pentylcarbamoyl)-ethyl)naphthalen-1-yl](ethoxyoxalyl)amino}benzoic acid (**11**) (950 mg) in methanol (7 mL) at ambient temperature was added 1 N NaOH (3.9 mL, 3.9 mmol). The basic mixture was stirred at ambient temperature for 2 h, and then 1 N HCl (10 mL) was added. The product was purified by reverse phase preparative HPLC to provide 210 mg of compound **3** as a light brown solid (0.39 mmol, 29% yield over two steps):

^{1}H NMR (400 MHz, DMSO-d_6) (mixture of rotamers) δ 13.13 (s, 1H), 8.43 (t, 1H, J = 7.8 Hz), 8.32 (d, 1H, J = 8.4 Hz), 8.22 (dd, 1H, J = 2.8, 8.4 Hz), [8.18 (d, J = 8.4 Hz), 8.08 (d, J = 8.4 Hz), 1H in total], 8.01−7.83 (m, 3H), 7.75−7.12 (m, 5H), 6.86−6.80 (m, 1H), 4.58 (q, 1H, J = 7.4 Hz), 3.67−2.82 (m, 6H), [(1.81, s), (1.78, s) (1.75, s), 3H in total], 1.39−1.00 (m, 4H), 0.92−0.69 (m, 3H); ^{13}C NMR

(40) Dygos, J. H.; Yonan, E. E.; Scaros, M. G.; Goodmonson, O. J.; Getman, D. P.; Periana, R. A.; Beck, G. A. *Synthesis* **1992**, 741.

(100 MHz, DMSO-d_6) (mixture of rotamers) δ (170.6 and 170.4), (169.2 and 169.1), (167.3 and 166.6), (163.5 and 163.1), 162.3, (138.6 and 138.5), (136.1 and 135.8), 137.2, (135.3 and 135.2), (133.2, 132.9, and 132.5), (132.0 and 131.9), 131.4, (130.3 and 130.2), (128.9 and 128.5), 127.9, (127.4 and 127.4), (126.7 and 126.6), 126.4, (125.2 and 124.9), 124.5, (124.4 and 124.2), (53.4 and 53.3), (38.5 and 38.4), (35.4 and 35.0), 28.5, (28.4 and 28.4), (22.5 and 22.4), 21.6, 13.8; MS (ESI) *m*/*z* 534 ([M + H]$^+$).

***S*-3-(4-Aminonaphthalen-1-yl)-2-(*tert*-butoxycarbonylamino)propionic Acid Methyl Ester (16).** To a mixture of 3.00 g (9.11 mmol) of *N*-(*tert*-butoxycarbonyl)-3-iodo-L-alanine methyl ester and 3.57 g (54.6 mmol) of zinc dust was added 10 mL of DMF.[41] The mixture was purged with N_2 and then heated at 65 °C for 15 min. The disappearance of the starting iodide was monitored by quenching an aliquot in 1 M HCl, then extracting the acid solution with ethyl acetate, and TLC analysis of the organic layer, eluting with 20% EtOAc/hexanes. After the iodide had been consumed, the excess zinc was allowed to settle, and the organozinc solution was added via syringe to a stirred and N_2-purged solution of 2.02 g (9.11 mmol) of 4-bromo-1-naphthylamine, 556 mg (1.82 mmol) of tris(*o*-tolyl)phosphine, and 100 mg (0.450 mmol) of palladium(II) acetate in 5 mL of DMF. The reaction was stirred at 65 °C for 1.5 h and then poured into 50 mL of water and extracted with diethyl ether (3 × 15 mL). During the first extraction, the mixture was filtered through diatomaceous earth to remove the insoluble zinc salts and precipitated palladium. The combined ether layers were back-extracted with water (1 × 15 mL) and brine (1 × 15 mL), dried over $MgSO_4$, filtered, and concentrated to a gummy residue. This was purified via silica gel chromatography, eluting with 40% ethyl acetate/hexanes to give 1.45 g (46%) of 3-(4-aminonaphthalen-1-yl)-2-(*tert*-butoxycarbonylamino)propionic acid methyl ester as a yellow foam. The product contained a minor higher R_f impurity that could be removed during the next step: ^{1}H NMR (400 MHz, $CDCl_3$) δ 8.01 (d, 1H, J = 8.3 Hz), 7.84 (d, 1H, J = 8.3 Hz), 7.52 (t, 1H, J = 7.2 Hz), 7.46 (t, 1H, J = 7.4 Hz), 7.07 (d, 1H, J = 7.7 Hz), 6.69 (d, 1H, J = 7.7 Hz), 5.02 (bd, 1, J = 8.0 Hz), 4.64 (bq, 1H, J = 6.1 Hz), 4.20 (bs, 2H), 3.61 (s, 3H), 3.47 (dd, 1H, J = 14.2, 6.0 Hz), 3.36 (dd, 1H, J = 14.0, 6.0 Hz), 1.40 (s, 9H); ^{13}C NMR (100 MHz, $CDCl_3$) δ 172.8 (C), 155.0 (C), 141.7 (C), 132.9 (C), 128.0 (CH), 126.2 (CH), 124.7 (CH), 124.2 (CH), 124.1 (C), 122.7 (C), 121.5 (CH), 109.2 (CH), 79.8 (C), 54.5 (CH or CH_3), 52.0 (CH_3 or CH), 35.2 (CH_2), 28.3 (CH_3); MS (ESI) *m*/*z* 245 ([M − Boc + 2H]$^+$), 345 ([M + H]$^+$), 367 ([M + Na]$^+$).

***S*-3-(4-Aminonaphthalen-1-yl)-2-(*tert*-butoxycarbonylamino)propionic Acid (17).** To a solution of 1.26 g (3.66 mmol) of 3-(4-aminonaphthalen-1-yl)-2-(*tert*-butoxycarbonylamino)propionic acid methyl ester (**16**) in 5 mL of CH_3OH was added 1.5 mL of 4 M NaOH(aq). The reaction was stirred at ambient temperature for 2.5 h and then concentrated in vacuo to an oil. This was diluted with 20 mL of water and extracted with diethyl ether (3 × 5 mL). The aqueous layer was cooled with an ice bath and stirred vigorously, 10 mL of ethyl acetate was added, and then 6 mL of 1 M HCl was added immediately. The layers were separated, and the aqueous layer was extracted with additional ethyl acetate (2 × 10 mL). The combined ethyl acetate layers were back-extracted with brine (1 × 10 mL), dried over $MgSO_4$, filtered, and concentrated in vacuo to 1.10 g (91%) of a tan solid: ^{1}H NMR (300 MHz, DMSO-d_6) δ 8.08 (d, 1H, J = 8.1 Hz), 7.94 (d, 1H, J = 8.5 Hz), 7.48 (ddd, 1H, J = 7.1, 6.8, 1.4 Hz), 7.38 (ddd, 1H, J = 7.5, 6.8, 0.9 Hz), 7.13 (d, 1H, J = 7.8 Hz), 7.10 (d, 1H, J = 9.5 Hz), 6.58 (d, 1H, J = 7.5 Hz), 4.11 (m, 1H), 3.39 (dd, IH, J = 14.4, 4.4 Hz), 3.02 (dd, 1H, J = 14.2, 10.2 Hz), 1.30 (s, 9H); ^{13}C NMR (100 MHz, $CDCl_3$) δ 174.2 (C), 141.4 (C), 135.9 (C), 132.9 (C), 128.0 (CH), 126.1 (CH), 124.6 (CH), 124.3 (CH), 124.2 (C), 123.2 (C), 121.4 (CH), 109.5 (CH), 79.8 (C), 54.3 (CH), 34.8 (CH_2), 28.2 (CH_3); MS (ESI) *m*/*z* 231 ([M − Boc + 2H]$^+$), 331 ([M + H]$^+$), 353 ([M + Na]$^+$).

(41) Jackson, R. F. W.; Moore, R. J.; Dexter, C. *J. Org. Chem.* **1998**, *63*, 7875.

3-((5-Aminopentyl)oxy)naphthalene-2-carboxylic Acid Methyl Ester Hydrochloride (19). To an ice-cooled solution of 1.44 g (71.3 mmol) of 3-hydroxy-2-naphthoic acid methyl ester (**18**), 1.45 g (7.13 mmol) of 5-((*tert*-butoxycarbonyl)amino)-1-pentanol, and 1.87 g (7.13 mmol) of triphenylphosphine in 15 mL of THF was added 1.2 mL (7.62 mmol) of diethylazodicarboxylate. The reaction was stirred and allowed to warm to ambient temperature over 15 h. The solvent was removed in vacuo, and then the thick oily residue was stirred with 15 mL of 30% ethyl acetate/hexanes to precipitate triphenylphosphine oxide. The precipitate was filtered away and washed with 5 mL of 30% ethyl acetate/hexanes, and then the combined filtrate and washings were concentrated to an oil. This was purified by silica gel chromatography, eluting with 30% ethyl acetate/hexanes to give 1.54 g (56%) of a pale yellow oil: ^{1}H NMR (400 MHz, $CDCl_3$) δ 8.28 (s, 1H), 7.80 (d, 1H, J = 8.0 Hz), 7.70 (d, 1H, J = 8.0 Hz), 7.49 (ddd, 1H, J = 7.1, 6.8, 1.2 Hz), 7.35 (ddd, 1H, J = 7.1, 7.1, 0.9 Hz), 7.17 (s, 1H), 4.66 (bs, 1H), 4.13 (t, 2H, J = 6.3 Hz), 3.94 (s, 3 Hz), 3.17 (brq, 2H, J = 5.2 Hz), 1.90 (m, 2H), 1.59 (m, 4H); ^{13}C NMR (100 MHz, $CDCl_3$) δ 166.8 (C), 156.0 (C), 155.0 (C), 136.1 (C), 132.6 (CH), 128.6 (CH), 128.3 (CH), 127.5 (C), 126.4 (CH), 124.3 (CH), 122.1 (C), 107.7 (CH), 79.0 (C), 68.4 (CH_2), 52.1 (CH_3), 40.4 (CH_2), 29.6 (CH_2), 28.6 (CH_2), 28.4 (CH_3), 23.2 (CH_2); MS (ESI) *m*/*z* 288 ([M − Boc + 2H]$^+$), 388 ([M + H]$^+$), 410 ([M + Na]$^+$).

The oil was dissolved in 10 mL of 4 M HCl in dioxane and stirred at ambient temperature for 1.75 h. The solvent was removed in vacuo to give 1.23 g (95%) of 3-((5-aminopentyl)oxy)naphthalene-2-carboxylic acid methyl ester hydrochloride as a light yellow solid: ^{1}H NMR (400 MHz, DMSO-d_6) δ 8.23 (s, 1H), 8.01 (bs, 3H), 7.93 (d, 1H, J = 8.0 Hz), 7.84 (d, 1H, J = 8.3 Hz), 7.54 (ddd, 1H, J = 7.1, 6.8, 1.2 Hz), 7.45 (s, 1), 7.39 (ddd, 1H, J = 7.1, 6.8, 1.1 Hz), 4.12 (t, 2H, J = 6.3 Hz), 3.85 (s, 3H), 2.79 (t, 2H, J = 7.7 Hz), 1.79 (m, 2H), 1.65 (m, 2H), 1.52 (m, 2H); ^{13}C NMR (100 MHz, DMSO-d_6) δ 166.2 (C), 154.0 (C), 135.5 (C), 131.2 (CH), 128.4 (CH), 128.2 (CH), 127.0 (C), 126.4 (CH), 124.3 (CH), 122.3 (C), 107.7 (CH), 67.8 (CH_2), 52.0 (CH_3), 38.6 (CH_2), 27.9 (CH_2), 26.5 (CH_2), 22.4 (CH_2); MS (ESI) *m*/*z* 288 ([M + H]$^+$).

***S*-3-{[5-[(3-(4-Aminonaphthalen-1-yl)-2-(*tert*-butoxycarbonylamino)propionyl)amino]pentyl]oxy}naphthalene-2-carboxylic Acid Methyl Ester (20).** To 510 mg (1.54 mmol) of acid **17**, 413 mg (2.16 mmol) of 1-(3-(dimethylamino)propyl)-3-ethylcarbodiimide hydrochloride (EDCI), and 208 mg (1.54 mmol) of 1-hydroxybenzotriazole was added 12 mL of CH_2Cl_2 and then 350 μL (3.18 mmol) of *N*-methylmorpholine. The solution was stirred at ambient temperature for 10 min, and then 500 mg (1.54 mmol) of amine−HCl **19** was added. The solution was stirred at ambient temperature for 19 h and then concentrated in vacuo. The residue was taken up in 20 mL of ethyl acetate and then extracted with water (2 × 10 mL), saturated $NaHCO_3$(aq) (2 × 10 mL), and brine (1 × 10 mL), dried over $MgSO_4$, filtered, and concentrated to a thick oil. The product was purified via silica gel chromatography, eluting with 60% ethyl acetate/hexanes to give an oil. Trituration with a small amount of diethyl ether followed by rapid evaporation in vacuo gave 480 mg (52%) of the amide as a light brown foam: ^{1}H NMR (400 MHz, $CDCl_3$) δ 8.27 (s, 1H), 8.14 (d, 1H, J = 8.3 Hz), 7.81 (d, 1H, J = 8.3 Hz), 7.78 (d, 1H, J = 8.6 Hz), 7.72 (d, 1H, J = 8.0 Hz), 7.51 (t, 2H, J = 7.5 Hz), 7.40 (t, 1H, J = 7.4 Hz), 7.37 (dt, 1H, J = 7.1, 0.9 Hz), 7.15 (s, 1H), 7.11 (d, 1H, J = 7.4 Hz), 6.64 (d, 1H, J = 7.7 Hz), 5.47 (bs, 1H), 5.36 (bs, 1H), 4.39 (bq, 1H, J = 6.5 Hz), 4.01 (t, 2H, J = 6.3 Hz), 3.90 (s, 3H), 3.47 (m, 1H), 3.27 (m, 1H), 3.05 (m, 2H), 1.74 (m, 2H), 1.41 (bs, 9H), 1.24 (m, 2H); ^{13}C NMR (100 MHz, $CDCl_3$) δ 171.2 (C), 166.6 (C), 155.3 (C), 155.0 (C), 141.6 (C), 136.1 (C), 132.6 (CH), 128.7 (CH), 128.4 (CH), 128.3 (CH), 127.5 (C), 126.3 (CH), 124.7 (CH), 124.4 (CH), 124.3 (CH), 124.0 (C), 123.4 (C), 122.0 (C), 121.4 (CH), 109.3 (CH), 107.6 (CH), 79.8 (C), 68.3 (CH_2), 55.8 (CH), 52.2 (CH_3), 39.1 (CH_2), 36.4 (CH_2), 28.5 (CH_2), 28.3 (CH_2), 28.3 (CH_3), 23.0 (CH_2); MS (ESI) *m*/*z* 500 ([M − Boc + 2H]$^+$), 600 ([M + H]$^+$), 622 ([M + Na]$^+$).

Chart 1.

```
-4    1
GFSH  MEMEKEFEQI DKSGSWAAIY QDIRHEASDF PCRVAKLPKN KNRNRYRDVS  50
      PFDHSRIKLH QEDNDYINAS LIKMEEAQRS YILTQGPLPN TCGHFWEMVW  100
      EQKSRGVVML NRVMEKGSLK CAQYWPQKEE KEMIFEDTNL KLTLISEDIK  150
      SYYTVRQLEL ENLTTQETRE ILHFHYTTWP DFGVPESPAS FLNFLFKVRE  200
      SGSLSPEHGP VVVHCSAGIG RSGTFCLADT CLLLMDKRKD PSSVDIKKVL  250
      LDMRKFRMGL IQTAEQLRFS YLAVIEGAKF IMGD 288
```

3-({5-[[2-(*tert*-Butoxycarbonylamino)-3-[4-((2-carboxyphenyl)-amino)naphthalen-1-yl]propionyl]amino]pentyl}oxy}naphthalene-2-carboxylic acid (21). To 382 mg (0.637 mmol) of aminonaphthalene **20**, 262 mg (0.766 mmol) of diphenyliodonium-2-carboxylate monohydrate (2), and 5 mg (0.028 mmol) of copper(II) acetate was added 3 mL of 2-propanol. The mixture was stirred at reflux under N_2 for 17 h and then concentrated in vacuo to a foam. This was taken up in 10 mL of ethyl acetate, then extracted with water (2 × 5 mL) and brine (1 × 5 mL), dried over $MgSO_4$, filtered, and concentrated to 481 mg (>100%) of a brown foam. The crude product contained some iodobenzene and a small amount of unreacted iodonium salt, but these did not interfere with the next reaction. Pure acid **21** could be obtained by silica gel chromatography, eluting with 50% ethyl acetate/hexanes to remove nonpolar impurities and then stepping to 75% ethyl acetate/hexanes to recover the product. From 100 mg of crude product and 30 mL of silica gel, 16 mg of pure acid **21** was obtained: ^{1}H NMR (400 MHz, DMSO-d_6) δ 10.03 (bs, 1H), 8.23 (d, 1H, J = 5.8 Hz), 8.22 (s, 1H), 7.99 (d, 1H, J = 8.6 Hz), 7.93 (m, 2H), 7.85 (m, 1H), 7.83 (d, 1H, J = 8.3 Hz), 7.61 (dt, 1H, J = 7.1, 1.2 Hz), 7.54 (m, 2H), 7.41 (m, 2H), 7.24 (t, 1H, J = 7.4 Hz), 6.91 (d, 1H, J = 8.6 Hz), 6.76 (d, 1H, J = 8.3 Hz), 6.71 (t, 1H, J = 7.7 Hz), 4.30 (m, 1H), 4.09 (t, 2H, J = 6.3 Hz), 3.83 (s, 3H), 3.49 (dd, 1H, J = 13.8, 5.2 Hz), 3.14 (m, 3H), 1.75 (m, 2H), 1.43 (m, 4H), 1.27 (bs, <9H), 0.98 (bs, minor rotamer); ^{13}C NMR (100 MHz, DMSO-d_6) δ 171.0 (C), 170.3 (C), 166.2 (C), 155.0 (C), 154.0 (C), 148.9 (C), 135.5 (CH), 135.0 (C), 133.8 (C), 132.8 (C), 131.7 (CH), 131.1 (CH), 131.0 (C), 129.2 (C), 128.4 (CH), 128.2 (CH), 127.6 (CH), 126.9 (C), 126.4 (CH), 126.3 (CH), 125.8 (CH), 124.5 (CH), 124.3 (CH), 122.5 (C), 122.4 (CH), 120.0 (CH), 116.6 (CH), 113.5 (CH), 112.1 (C), 107.6 (CH), 77.9 (C), 68.0 (CH_2), 55.3 (CH), 51.9 (CH_3), 38.4 (CH_2), 35.1 (CH_2), 28.6 (CH_2), 28.1 (CH_2), 28.0 (CH_3), 27.5 (CH_3, minor), 22.7 (CH_2); MS (ESI) m/z 620 ([M − Boc + 2H]$^+$), 720 ([M + H]$^+$), 742 ([M + Na]$^+$).

3-({5-[(*N*-Acetyl-3-{4-[(carboxycarbonyl)(2-carboxyphenyl)amino]-1-naphthyl}-L-alanyl)amino]pentyl}oxy)-2-naphthoic Acid (23). To an ice-cooled solution of 100 mg (0.139 mmol) of amino acid **21** in 1 mL of DMF was added 200 μL (1.44 mmol) of triethylamine and then 100 μL (0.90 mmol) of ethyl chlorooxoacetate. The ice bath was removed, and the reaction was stirred at ambient temperature for 2 h. Next, 2 mL of 2 M NaOH was added, along with 5 mL of water. After being stirred for another 2 h, the reaction was diluted with 10 mL of water, and stirred again for 2 h. The reaction was monitored for disappearance of the less polar naphthoic ester by reverse-phase analytical HPLC. Additional 2 M NaOH could be added if hydrolysis was incomplete, though a total of 3 mL of 2 M NaOH was sufficient to complete the hydrolysis. The reaction was cooled with an ice bath, and then 3 mL of 6 M HCl was added. The mixture was extracted with ethyl acetate (3 × 5 mL) and then the combined ethyl acetate layers were back-extracted with water (2 × 5 mL) and brine (1 × 5 mL), dried over $MgSO_4$, filtered, and concentrated to a foam containing crude oxamic acid **22**. This was dissolved in 1 mL of trifluoroacetic acid and allowed to stand at ambient temperature for 10 min. The trifluoroacetic acid was removed in vacuo, and the resulting foam was taken up in 3 mL of 2 M NaOH. To the basic solution was added 300 μL of acetic anhydride, and the mixture was stirred at ambient temperature for 30 min, after which the pH = 7. A small amount of insoluble material was filtered away, and then the product was isolated by reverse phase HPLC, eluting with a 0−70% acetonitrile in 0.1% (v/v) aqueous trifluoroacetic acid gradient to give 28 mg (28%) of compound **23** as a light yellow solid. The enantiomeric purity of compound **23** was determined to be 100% by chiral HPLC. The synthesis of *ent*-**23** was accomplished according to the same sequence but starting with *N*-(*tert*-butoxycarbonyl)-3-iodo-D-alanine methyl ester to prepare *ent*-**16**. Both enantiomers were treated with diazomethane and then evaluated using a ChiralPak AS column from Chiral Technologies (4.6 × 250 mm, 10 μm), eluting with 30% 2-propanol/hexanes. t_R for **23** = 9.9 min, and t_R for *ent*-**23** = 15.8 min. ^{1}H NMR (500 MHz, DMSO-d_6): mixture of rotamers, δ 8.45−8.42 (m, 1H), 8.35−8.30 (m, 1H), 8.26−8.21 (m, 1H), 8.18 (s, 1H), 8.06−7.95 (m, 2H), 7.92 (d, 1H, J = 8.2 Hz), 7.84 (m, 2H), 7.67−7.47 (m, 5H), 7.17 (m, 1H), 6.83 (t, 1H, J = 6.4 Hz), 4.70−4.58 (m, 1H), 4.07 (t, 1H, J = 6.4 Hz), 4.03 (t, 1H, J = 6.4 Hz), 3.59−2.99 (m, 4H), 2.07 (s, 3H), 1.80−1.63 (m, 4H), 1.39−1.16 (m, 5H). MS (ESI): m/z 720 ([M + H]$^+$), 742 ([M + Na]$^+$).

Protein NMR Spectroscopy. Human PTP1B (residues 1−288) was cloned into the pGEX-5X vector (Amersham Pharmacia) and expressed in *Escherichia coli* BL21(DE3) cells. The final protein construct used for the NMR studies was 292 residues comprised of the following amino acid sequence shown in Chart 1. Two point mutations exist in the construct (E252D and D265E, underlined), along with four additional N-terminal residues (GFSH) that remain after cleavage of the GST-fusion.

Uniformly ^{15}N-labeled and $^{13}CH_3$(IVLM)-labeled PTP-1B was prepared by growing the bacteria on a minimal medium containing 1 g/L of $^{15}NH_4Cl$ (Cambridge Isotopes) or by adding 100/100/50 mg/L of ^{13}C-γ-methionine/3,3′-^{13}C-α-ketovalerate/3-^{13}C-α-ketobutyrate[24] 1 h before induction with 1 mM IPTG, respectively. Carbenicillin (0.1 mg/mL) was used as the selection agent. In addition to the standard salts, metals, and vitamins, the media contained the following additives (g/L of culture): Ala (0.5); Arg (0.4); Asp (0.4); Cys (0.05); Glu (0.65); Gln (0.4); Gly (0.55); His (0.1); Lys (0.42); Phe (0.13); Pro (0.1); Ser (2.1); Thr (0.23); Tyr (0.17); adenine (0.5); guanosine (0.65); thymine (0.2); uracil (0.5); cytosine (0.2); sodium acetate (1.5); succinic acid (1.5). The cell pellets were resuspended in a buffer containing 10 mM sodium phosphate (pH 7.4) and 150 mM NaCl (PBS buffer). The cells were then lysed using a microfluidizer (Microfluidics International) and the resulting lystate clarified via centrifugation at 76 000g for 10 min. The clarified cell lysate was loaded onto a Glutathione Sepharose 4B column (Pharmacia), and the resin was washed with 20 column volumes of PBS buffer. The protein was eluted with 5 column volumes of a buffer containing 50 mM TRIS (pH 8.0) and 10 mM reduced glutathione. The N-terminal GST fusion was cleaved with thrombin (1 U thrombin/mg of PTP-1B) at 4 °C for 72 h. Cleavage was monitored by SDS−PAGE analysis. The resulting solution was then concentrated and dialyzed to remove the glutathione (final dilution factor of 10^{-10}) and loaded onto a Glutathione Sepharose 4B column to remove the GST. The flow-through (containing PTP-1B) was collected and dialyzed against NMR buffer (see below). Typical protein yields were 10−20 mg of PTP-1B/L of culture.

The NMR samples were composed of uniformly ^{15}N-labeled or $^{13}CH_3$(IVLM) PTP-1B in an H_2O/D_2O (9/1) TRIS buffered solution (25 mM, pH = 7.5) containing DTT (10 mM). Ligand binding was detected by acquiring sensitivity-enhanced ^{1}H/^{15}N- or ^{1}H/^{13}C-HSQC spectra[42,43]

(42) Kay, L. E.; Keifer, P.; Saarinen, T. *J. Am. Chem. Soc.* **1992**, *114*, 10663.
(43) Stonehouse, J.; Shaw, G. L.; Keeler, J.; Laue, E. D. *J. Magn. Reson.* **1994**, *107*, 178.

on 400 μL of PTP-1B in the presence and absence of added compound. Protein concentrations were 300 and 25 μM for the ^{15}N- and $^{13}CH_3$-(IVLM)-labeled samples, respectively. A Bruker sample changer was used on a Bruker AMX500 spectrometer equipped with a cryoprobe.[44] Compounds were individually tested at concentrations of 0.1−15.0 mM, and binding was determined by monitoring changes in the HSQC spectra. Dissociation constants were obtained for selected compounds by monitoring the chemical shift changes of the protein resonances as a function of ligand concentration. Data were fit using a single binding site model. A least-squares grid search was performed by varying the values of K_D and the chemical shift of the fully saturated protein.

X-ray Crystallography. The final concentration of the purified protein sample was 3−4 mg/mL and contained various amounts of reducing agents, normally 2−4 mM DTT. Crystals of PTP1B (residues 1−321) belonging to space group $P3_121$ ($a = b = 88.4$ Å, $c = 104.5$ Å) were grown routinely using the protocol described by Puius[31] with the following changes. The buffers used in protein crystallization were degassed for approximately 30 min and then purged with argon gas prior to their use for crystallization. This simple precaution extended the lifetime of the reactive cysteine (Cys215) in the active site and provided a more stable and structurally homogeneous conformation of the active site. This protocol allowed the soaking of all the PTP1B inhibitors directly into the crystals. Soaking times ranged from one to 5 h and were normally no more that 2 h. Soaking was performed using 50 μL of the reservoir in the crystallization well and mixed with a 2−4 μL of stock (DMSO) solution of the compound at 100 mM concentration. The soaking protocol permitted the rapid structure determination of PTP1B:inhibitor complexes.

After the soaking period, crystals were transferred to a cryoprotectant solution for 5−10 s with rayon loops and exposed to the X-rays. The cryoprotectant solution consisted of 100 mM HEPES and 0.2 M magnesium acetate adjusted to pH 7.1 with NaOH at a 16% w/v concentration of PEG8000 with a 35% v/v concentration of glycerol. Crystallographic data were collected both in a conventional, in-house, protein crystallography laboratory and at sector 17 at the Advanced Photon Source (ID and BM lines of IMCA-CAT). Conventional sources were used routinely. The data collection hardware were a Mar Research Image Plate (180 mm), a Mar Research 345 mm image plate, or a Mar Research 165 mm CCD detector, all driven by the manufacturer's software. For a complete data set, 80−100 1° frames were collected at a crystal to detector distance of 80−90 mm. Exposure times were typically 10 min/frame for in-house data collection and 10 s for the synchrotron source. This strategy resulted in >96% completeness in the vast majority of the data sets with reducing *R*-factors between 5 and 9%. Data were processed with HKL2000 and scaled with SCALEPACK or within HKL2000. Phase and map calculations were performed using XPLOR or CNX. The modeling and electron-density fitting software QUANTA was used to manipulate the models. Refined crystallographic coordinates for the structure of hPTP1B complexed with compounds **5**, **12**, and **23** have been deposited with the Protein Data Bank (www.rcsb.org) with entry codes 1NO6, 1NL9, and 1NNY, respectively.

Biological Assay. Protein tyrosine phosphatase 1B (PTP1B) activity was determined by measuring the rate of hydrolysis of a surrogate substrate, *p*-nitrophenyl phosphate (*p*NPP, C1907 Sigma, St. Louis, MO). The assay was carried out at room temperature in 96 well polypropylene or polyethylene plates in a total volume of 100 μL/well. Appropriate dilutions of the compounds were made in DMSO and then diluted 10-fold into assay buffer (25 mM HEPES (pH = 7.5), 150 mM NaCl, and 0.1 mg/mL BSA). A 10 μL volume of 5 different concentrations of the test compound (inhibitor) or 10% DMSO in assay buffer was added to individual wells containing 40 μL of 3.2, 8, 20, and 50 mM *p*NPP in water. The reaction was initiated by adding 50 μL of PTP1B diluted in 2× assay buffer (50 mM HEPES, 300 mM NaCl, and 0.2 mg/mL BSA). The phosphatase activity resulted in the formation of the colored product *p*-nitrophenol (*p*NP) which was continuously monitored at 405 nm every 30 s for 15 min using an appropriate plate reader. The absorbance at 405 nm was converted to nanomoles of *p*NP using a standard curve, and the initial rate of *p*NP formation was calculated. For each concentration of test compound (inhibitor) or DMSO control, the initial rates were used to fit the rectangular hyperbola of Michaelis−Menten by nonlinear regression analysis (GraphPad Software Prism 3.0). The ratio of the apparent K_m/V_{max} vs inhibitor concentration was plotted, and the competitive K_i was calculated by linear regression to be the negative *x*-intercept. The uncompetitve K_i was similarly calculated from the *x*-intercept of the plot of the reciprocal of the apparent V_{max} versus the inhibitor concentration.[27]

Acknowledgment. The authors thank Jamey Mack for preparation of the ^{13}C methyl-labeled PTP1B for NMR-based screening and Mark Mullally for determining the enantiomeric purity of inhibitor **23**.

Supporting Information Available: Kinetic data of inhibition for naphthyloxamic acid **5**. This material is available free of charge via the Internet at http://pubs.acs.org.

JA0296733

(44) Hajduk, P. J.; Gerfin, T.; Boehlen, J.-M.; Häberli, M.; Marek, D.; Fesik, S. W. *J. Med. Chem.* **1999**, *42*, 2315.